

CHARACTERIZATION OF EMERALDS FROM A HISTORICAL DEPOSIT: BYRUD (EIDSVOLL), NORWAY

Benjamin Rondeau, Emmanuel Fritsch, Jean-Jacques Peucat,
Fred Steinar Nordrum, and Lee Groat

An emerald deposit at Byrud, in southern Norway, yielded significant quantities of crystals and gem rough in the late 19th and early 20th centuries. Complex multiphase inclusions in the emeralds consist of water, gaseous methane, halite, sylvite, calcite, and a sulfide assemblage (pyrrhotite, galena, and sphalerite). This sulfide assemblage makes it easy to distinguish Byrud emeralds from those from other localities with a binocular microscope. The chemical composition of Byrud emeralds is also characteristic: They are colored mostly by vanadium (up to 1 wt.% V_2O_3), and contain low sodium and magnesium (0.1 wt.% oxide or less). Moreover, the relative amounts of iron, magnesium, chromium, rubidium, and cesium appear to be diagnostic. Infrared absorption spectra show that they contain little water. Emeralds from the Byrud deposit are still occasionally recovered by hobbyist collectors from the mine dumps.

During the late 19th and early 20th centuries, the Byrud emerald deposit in Norway was mined commercially and produced many fine specimens (e.g., figure 1), as well as a limited amount of gem rough. Some of the crystals are housed in museum collections around Europe, and it is not uncommon to encounter a Byrud emerald in an antique jewelry piece. The mine is located on the shore of Lake Mjøsa, near Minnesund and a short distance from Eidsvoll, about 60 km north-northeast of Oslo, Norway (figure 2). The history, geology, and mineralogy of the deposit were comprehensively described by Nordrum and Raade (2006), and are summarized here. The aim of the present article is to characterize the emeralds from Byrud to make their unambiguous identification possible.

From a geologic and spectroscopic standpoint, emeralds from Byrud are interesting because they are vanadium-rich, as is also the case for emeralds from Colombia and some (or all) emeralds from a number of other deposits: Lened in the Northwest Territories, Canada; Salininha in Bahia, Brazil; Ma-

lipo in Yunnan, China; Panjshir, Afghanistan; and Gandao, Pakistan. In this article, we refer to “vanadian emeralds” as those that contain more vanadium than chromium, even when the vanadium content is somewhat low. The mechanisms of beryl coloration by Cr and V are very similar (Burns, 1993; Schwarz and Schmetzer, 2002); in 1988, after many years of controversy, vanadium joined chromium as an accepted coloring agent for emerald (CIBJO, 1988).

HISTORICAL BACKGROUND

The Byrud emerald deposit was probably discovered in the 1860s. During these early years, emerald specimens were obtained by several European natural history museums, including Stockholm in

See end of article for About the Authors and Acknowledgments.
GEMS & GEMOLOGY, Vol. 44, No. 2, pp. 108–122.
© 2008 Gemological Institute of America



Figure 1. This 1.1-cm-long gem-quality emerald crystal on matrix, which was found by a collector at Byrud in the 1980s, is typical of emeralds from this locality. It is accompanied by quartz, feldspar, spheres of muscovite, and grayish fluorite. Courtesy of the Norwegian Mining Museum, Kongsberg; photo by Rainer Bode.

1868, Oslo in 1869, and London in 1870. Websky (1876) first described the morphology of the Byrud emeralds, and stated that the deposit was of commercial importance.

Preliminary prospecting and blasting took place around 1880 (Bull, 1952). Evelyn Aston inspected the almost forgotten occurrence in November 1898; at that time, the old workings consisted of an opening 2 m high and 1 m wide that accessed a room measuring about 3.5 m in diameter. On her next visit, she brought a miner who blasted further, and they found gem-quality emerald crystals in small clay-filled pockets (Cameron, 1963).

On April 5, 1899, the prospect (called Narum) was purchased by Evelyn's father, English mining prospector Edward Y. Aston. A London-based company—the Norwegian Exploration Co. Ltd.—was registered May 9, with Aston as a major shareholder in exchange for the property and rights to the emerald occurrence, as well as some additional prospects. Mining began in spring 1899 (figure 3). In June 1900, the company was renamed the Norwegian & General Exploration Co.

Ltd. Edward Aston died on September 21, 1900, and on December 28, 1907, the company was liquidated and the assets sold to the Cornish Development Co. Ltd. The mine was subsequently abandoned in 1909 (Nordrum and Raade, 2006).

In the first years of mining, up to 30 miners were employed at Byrud. A crusher, washing plant, blacksmith's forge, administration building, and a small workshop were reportedly built at the mine, but few vestiges are visible today. However, production could not sustain this level of mining for very long, and by the time the mine closed 10 years later, it had only nine employees. It does not appear that the mine was ever profitable, even during the first few years (Nordrum and Raade, 2006).

Nevertheless, many gem-quality emeralds were recovered, some of which were displayed at the Paris World's Fair in 1900. Besides crystals, wrote Kunz (1902, p. 742), "Many cut stones, most of them pale in color, but generally free from flaws, were shown." Sinkankas (1981, p. 487) stated: "Only rarely were good stones found and then never



Figure 2. The Byrud emerald deposit is located on the western shore of Norway's Lake Mjøsa, close to Minnesund and a short distance from Eidsvoll, in southeastern Norway. Adapted with permission from Mineralien Welt (Nordrum and Raade, 2006, p. 52).

Figure 3. Commercial mining of the Byrud emerald deposit began in 1899, when this photo was taken. This building has since disappeared, but the tunnels are still visible. Courtesy of the Aston family archives.



more than about 6 mm in diameter, but the color quality was considered to be of the highest grade, and if anything a little too bluish. Selset (1963) cut some of the crystals himself and claimed that the gems matched the finest from any other source." Most of the transparent crystals from cavities were pale colored, but some were a fine, deep green. Cemented in feldspar, translucent crystals up to more than 1.2 cm in diameter and 5 cm in length with a deep green color were recovered. Translucent crystals were also commonly found in quartz.

A cut emerald from Byrud is said to have been used in a jewel belonging to the royal family of Great Britain, possibly in connection with the coronation of King Edward VII in 1902. The English companies sold the rough crystals and mineral specimens outside Norway, and no records of the sales have been found. The production data and names of the buyers are unknown (Nordrum and Raade, 2006).

Most of the emerald crystals pictured in this article were found by mineral collectors over the past 30 years (see, e.g., figure 4). For a small daily fee to the landowners, collectors have been allowed to search in the mine dumps. Several fine specimens and single crystals have been recovered over the years, but

the chances of making good finds are diminishing and gem-quality specimens are discovered only rarely today. The underground mine has not been worked since 1909.

GEOLOGY AND MINERALOGY

The emerald deposit is located in the northeastern part of the Oslo region, which is a rift structure of Permian age (Vogt, 1884; Goldschmidt, 1911; Nordrum and Raade, 2006). Flat-lying maenaite (syenitic) sills, usually ranging from 0.5 m to several meters thick, transect Cambrian alum shale (a black, clay-rich, iron sulfide-containing, carbonaceous sedimentary rock) over a distance of about 200 m. The sills generally dip 15–20° west but are nearly horizontal in places. They are present in at least three levels and have been intruded by small pegmatites, which also cross-cut the alum shales. Close to the pegmatites, the shales are often bleached. The pegmatites usually range from a few centimeters to 30 cm in thickness, but may locally reach up to 1 m. They form lenses or dikes that are commonly discontinuous and locally contain small cavities. The pegmatites have an alkali syenitic composition, consisting mainly of K-feldspar (microcline), and were intruded during the Permian Period in conjunction with alkaline magmatic activity in the area (Ihlen, 1978). A large alkaline granite intrusion occurs not far to the west of Byrud, and the pegmatites are most likely associated with this intrusive.

Emerald mining has taken place along the maenaite sills at various levels. Beryl occurs chiefly in the pegmatites (figure 5), and occasionally in the maenaites and in the shales adjacent to the pegmatites. The best-quality emeralds have been found in the northern part of the mining area (Lindaas, 1982), in small clay-filled pockets (Cameron, 1963). Vanadium and chromium, chromophores in the emeralds, were probably leached from the alum shales by the mineralizing fluids.

In addition to microcline, the pegmatites typically contain quartz and muscovite. Sodic plagioclase, pyrite, pyrrhotite, fluorite (purple and pale green), topaz, and beryl are also common in the pegmatites. Micro-crystals of laumontite and rutile (“ilmenorutile-strüverite”) are frequently present as well. Goethite, jarosite, and gypsum are common secondary minerals. In all, 45 minerals have been reported from this deposit (Nordrum and Raade, 2006; Kvamsdal and Eldjarn, 2007). A complete list of minerals associated with the emerald mineral-

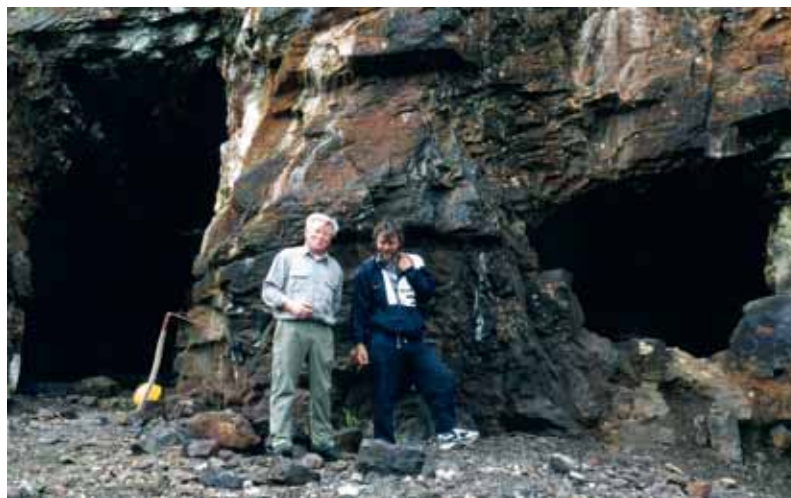


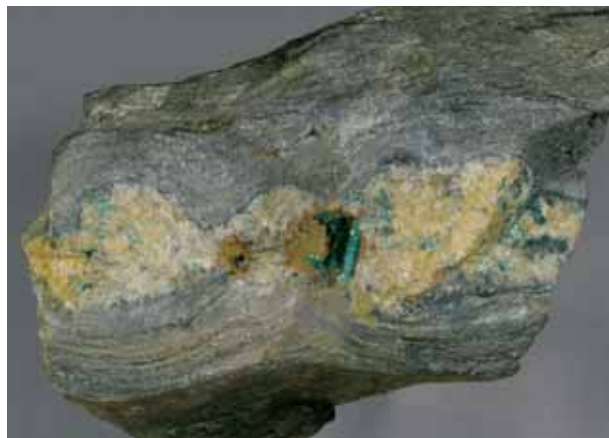
Figure 4. Galleries excavated for emerald extraction during the late 19th and early 20th centuries are still visible. Mineral collectors, such as Arnfinn Juliussen and Bjørn Skår in this photo, can visit the mine with the permission of the owners, Anne Grethe Røise and Ole Jørgen Bjørnstad. Photo by F. S. Nordrum.

ization is available on the G&G Data Depository (www.gia.edu/gemsandgemology).

MATERIALS AND METHODS

The authors studied three emerald-in-matrix specimens, collected more than a century ago, from the mineralogy collection of the Muséum National d'Histoire Naturelle (National Museum of Natural History) in Paris (collection nos. 106.718, 195.174,

Figure 5. Byrud emerald crystals are found mainly in small pegmatites intruding alum shales. This sample is 9.5 cm long, and the emerald crystals attain lengths of 9 mm. Courtesy of the Norwegian Mining Museum; photo by Gunnar Jensen.



and 203.18). These idiomorphic bluish green crystals, each a few millimeters in length, are intergrown with feldspar, quartz, muscovite, and purple fluorite. One emerald crystal was removed from each of the matrix specimens and all three were polished to measure their gemological, chemical, and spectroscopic properties. In addition, we studied four loose transparent crystals, each measuring a few millimeters in length, that were recovered in the 1980s and belong to the collection of the Norwegian Mining Museum in Kongsberg (collection nos. BVM2378-A to D; figure 6). All seven samples studied were transparent and homogeneous in color, so we believe that they are representative of the material from which gems would be faceted. We did not study any cut stones or stones set in jewelry, as the very few that are known were not accessible.

Gemological data were acquired on various samples (see Results) using a Topcon refractometer, a 4-watt UV lamp with short-wave (254 nm) and long-wave (365 nm) bulbs, and an Olympus binocular microscope equipped with crossed polarizers and up to 1000× magnification. Specific gravity was determined by a combination of mass measurement using a precision scale and volume measurement using a classic pycnometer.

The composition of fluid inclusions in three samples (nos. 106.718, 195.174, and 203.18) was first determined by Raman spectroscopy using a

Jobin-Yvon T64000 dispersive spectrometer equipped with a confocal-type apparatus. The Ar⁺ laser (514 nm excitation) was operated with a power of 120 mW, and spectra were measured at a resolution of 2 cm⁻¹. Subsequently, one crystal (from sample 203.18) was broken to expose some of its fluid inclusions, and these were examined using a scanning electron microscope (SEM); the micro-crystals in about 30 of the inclusions were analyzed with an attached energy-dispersive spectrometer (EDS). We used a Zeiss Supra 55 VP SEM with an acceleration voltage of 7 or 22 kV, and a current of ~1 nA.

Electron-microprobe analyses of two samples (21 spots) were obtained with a fully automated Cameca SX-50 instrument, using the wavelength-dispersive mode with the following operating conditions: 15 kV excitation voltage, 20 nA beam current, 20 sec. peak count time, 10 sec. background count time, and 10 μm spot diameter. Data reduction was done using the "PAP" $\phi(\rho Z)$ method (Pouchou and Pichoir, 1991). Trace-element compositions of three emeralds (14 analyses) were measured using laser ablation-inductively coupled plasma-mass spectrometry (LA-ICP-MS) with an HP4500 spectrometer. The CETAC SLX200 ablation system used a Nd:YAG laser emitting at 1064 nm, frequency quadrupled to 266 nm. We limited our sampling to three emeralds, because this technique is somewhat destructive and cannot be applied to museum specimens.

Polarized ultraviolet-visible-near infrared (UV-Vis-NIR) absorption spectra of four samples (BVM2378-A to D) were acquired with a Varian Cary 5G spectrometer in the range 300–2500 nm, with a sampling interval of 1 nm and a spectral bandwidth of 1 nm, at a scan speed of 600 nm per minute, using 1 × 1 cm Glan-Thomson calcite polarizers. Infrared absorption spectra of three samples (nos. 106.718, 195.174, and 203.18) were acquired using a Nicolet 20SX spectrometer in the range 5800–1800 cm⁻¹. The spectra presented are directional (not polarized), with the beam (and not the electrical vector) parallel, and then perpendicular, to the optic axis.

RESULTS

Gemological Properties. Visual Appearance and Crystal Morphology. The emerald crystals were translucent to transparent and formed hexagonal crystals with flat basal terminations (figures 7 and 8). Pyramidal faces have also been seen on the terminations of Byrud emeralds (figure 8, right-hand crystal). The studied crystals were green to bluish green, and

Figure 6. These emerald crystals (sample nos. BVM2378-A to D), which are typical of those from Byrud, were characterized for this study. Note their rather homogeneous bluish green color. The longest crystal measures 9 mm. Photo by Alain Cossard.





Figure 7. This 1.2-cm-long emerald crystal is partially embedded in a spherulitic muscovite matrix. Courtesy of the Norwegian Mining Museum; photo by Gunnar Jenssen.

showed weak but significant pleochroism, from bluish green to yellowish green. All samples studied were homogeneous in color, though we have observed some crystals (not included in this study) that exhibit very strong color zonation parallel to the basal plane, with some parts nearly colorless (again, see figure 8).

Figure 8. These two Byrud crystals (not studied for this report) show unusual features. The 5-mm-long crystal on the left has distinct color zonation, while the crystal on the right (3.5 mm in diameter) has a complex termination consisting of pedion and pyramidal faces. Courtesy of Bjørn Skår; photo by O. T. Ljøstad.



Refractive Indices. We measured the refractive indices from the natural prism faces of samples BVM2378-A to D and obtained identical values of $n_o = 1.578$ and $n_e = 1.560$. Three crystals from sample 203.18 were polished parallel to the c-axis, and we measured $n_o = 1.587$ and $n_e = 1.579$. In all cases, the birefringence was 0.008.

Specific Gravity. We measured a specific gravity of 2.75 on five fragments of sample 203.18. Additional SG measurements could not be done because many samples were crystals on matrix (in particular, samples BVM2378-A to D contained too much matrix material on their extremities).

UV Fluorescence. All samples were inert to both short- and long-wave UV radiation, as with most natural emeralds worldwide (Bosshart, 1991; Zylbermann, 1998).

Magnification. In the seven emerald samples studied with a gemological microscope, we observed a few solid inclusions; these showed a bright yellow metallic luster and were most probably pyrite. All the samples contained primary fluid inclusions, virtually all of which were multiphase (figure 9). We observed no secondary inclusions. Some inclusions had an irregular outline (figure 10), and others showed a somewhat hexagonal outline when viewed parallel to the c-axis of the host (again, see figure 9), indicating that crystal growth occurred mostly along the basal planes.

Figure 9. Multiphase inclusions are commonly observed in emeralds from Byrud. They typically show regular geometric outlines and contain a liquid and a gaseous phase, a cubic transparent solid phase, elongated transparent crystals, and opaque phase(s). Photomicrograph by B. Rondeau; magnified 200 \times .



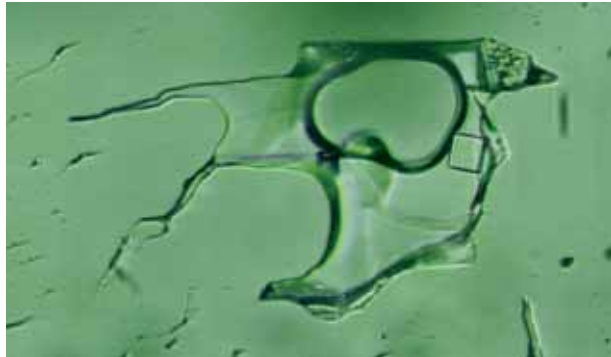


Figure 10. In rare instances, the multiphase inclusions in Byrud emeralds were observed to have irregular forms. Photomicrograph by B. Rondeau; magnified 500 \times .

The most characteristic multiphase inclusions (figure 11) contained predominantly a liquid phase, a gas bubble, an optically isotropic cube, some transparent, birefringent elongated material (as revealed between crossed polarizers, figure 11 right), and very small opaque phases. When these opaque phases are sufficiently large, one can see that they have a brownish yellow metallic luster (best observed using fiber-optic lighting from the side).

Composition of the Multiphase Inclusions. Raman Spectroscopy. Raman analyses revealed that the transparent cubes were halite and the aggregates of elongated opaque material were calcite (peaks at 1083, 279, 182, and 151 cm^{-1}). The liquid was water (broad band around 3600 cm^{-1}), and the gaseous phase was a mixture of water and methane (CH_4 ; broad band around 3600 cm^{-1} and sharp peak at 2915 cm^{-1}).

SEM-EDS Analysis. Fresh breaks on a fragment of sample 203.18 exposed numerous fluid inclusions. The liquid and gaseous phases were flushed out of the inclusions during sample preparation, and the solid phases were lost from some of the cavities as well. In those that still contained solids (figures 12 and 13), the most common phase identified was

halite (NaCl); sylvite (KCl) was also found frequently. Several sulfide phases were observed: pyrrhotite (Fe_{1-x}S , hexagonal flakes), galena (PbS), and sphalerite (ZnS); these were often grouped together (again, see figure 12). Copper was also detected during the analysis, but we could not ascribe it to a specific mineral. Some rarer solid phases were also identified. In particular, we found one cassiterite crystal (SnO_2) and one crystal of a phase that contained phosphorus, oxygen, and scandium that we attributed to the very rare mineral pretulite (ScPO_4 ; again, see figure 13).

Chemical Composition. Electron-microprobe analyses are summarized in table 1, and LA-ICP-MS analyses are provided in table 2; additional data from both techniques are available on the *G&G* Data Depository (www.gia.edu/gemsandgemology). We measured relatively high concentrations of V (up to 2.44 wt.% V_2O_3 , with a mean of more than 1 wt.%) and comparatively moderate concentrations of Cr (up to 0.33 wt.% Cr_2O_3). The V/Cr ratio was very high, ranging from 3.7 to 24.3. The emeralds also contained remarkably low concentrations of Mg and Na (about 0.1 wt.% oxide or less). Concentrations of Rb (21–61 ppm) and Cs (35–127 ppm) were quite high compared to other vanadian emeralds. Iron concentrations were low (467–1024 ppm) compared to emeralds from most other deposits.

Spectroscopy. UV-Vis-NIR. Typical polarized absorption spectra of a Byrud emerald (no. BVM2378-A) are presented in figure 14. The spectrum acquired with $E \perp c$ shows V- (and partially Cr-) related absorption bands at 430 and 608 nm. With $E \parallel c$, the spectrum shows absorption bands at 423 and 630–642 nm (compare to Fritsch et al., 2002). A weak absorption band at 683 nm (spectrum $E \parallel c$) is attributed to chromium. The weak shoulders at 373 and 385 nm are due to Fe^{3+} .

In the near-infrared region, the three main absorption bands at approximately 1150, 1400, and 1896 nm are due to type I and type II water.

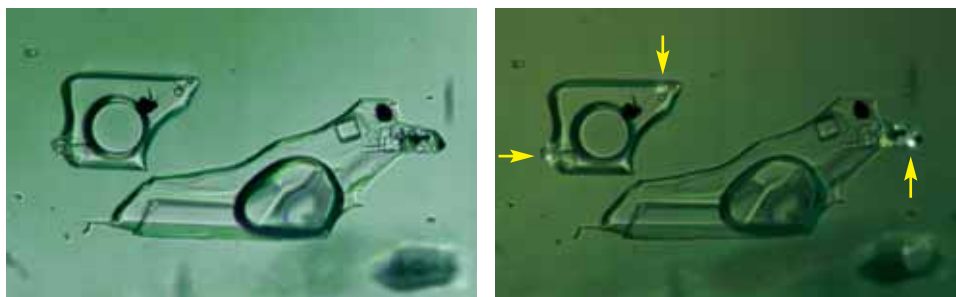


Figure 11. As shown in polarized light (left) and between partially crossed polarizers (right), the Byrud emerald's cubic phases are isotropic, whereas the elongated aggregates are anisotropic (yellow arrows). Note the opaque phases. Photomicrographs by B. Rondeau; magnified 500 \times .

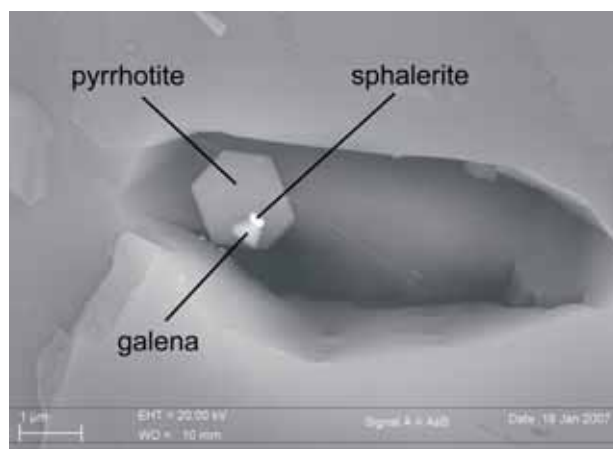


Figure 12. This multiphase inclusion in emerald sample 203.18 contains three sulfides: galena, sphalerite, and pyrrhotite. This assemblage is commonly found together in the multiphase inclusions within Byrud emeralds. Backscattered electron image.

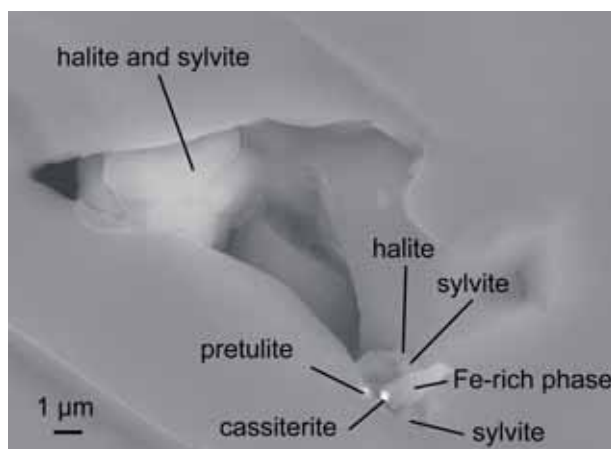


Figure 13. This inclusion in emerald sample 203.18 is a relatively rare example containing several phases including cassiterite (SnO_2) and pretulite (ScPO_4), as well as the common halite and sylvite. Backscattered electron image.

Infrared. Figure 15 shows two directional IR spectra in the $5800\text{--}1800\text{ cm}^{-1}$ range. Both H_2O and CO_2 absorptions are clearly visible. Details of the water-related absorptions in the range $4000\text{--}3000\text{ cm}^{-1}$ are given in figure 16. These spectra show typical absorptions due to both type I H_2O ($3700\text{--}3694$ and 3607 cm^{-1}) and type II H_2O (3657 and $3597\text{--}3595\text{ cm}^{-1}$) molecules. The peak at 5273 cm^{-1} ($\nu_2 + \nu_3$), attributed to type II water, is quite sharp and weak (figure 15), which means that there are relatively few type II water molecules in emeralds from Byrud.

Details of the absorptions in the $3000\text{--}2100\text{ cm}^{-1}$ range are given in figure 17. The CO_2 absorption at

2359 cm^{-1} is sharp; weak absorptions at 2372 , 2345 , and 2326 cm^{-1} are also attributed to CO_2 . These are possibly due to isotopic effects (combination of the presence of ^{13}C and ^{18}O). The weak peak at 2818 cm^{-1} is attributed to chlorine (Schmetzer et al., 1997, and references therein; Fritsch et al., 1998). Several additional peaks shown in figure 17 (i.e., at 2928 , 2854 , 2739 , 2687 , and 2640 cm^{-1}) have never before been documented in the literature for natural emeralds. They may correspond to companion peaks of the 2818 cm^{-1} chlorine peak, even if their positions differ slightly from those observed in hydrothermal synthetic emeralds.

TABLE 1. Chemical composition of two Byrud emeralds, obtained by electron microprobe.^a

Oxide (wt.%)	Sample 203.18			Sample 195.174		
	Range	Average	Std. dev.	Range	Average	Std. dev.
SiO_2	65.49–66.73	65.91	0.33	65.55–66.06	65.76	0.18
Al_2O_3	17.02–18.78	17.93	0.43	17.39–18.23	17.91	0.28
BeO^b	13.69–13.92	13.77	0.06	13.71–13.78	13.74	0.03
V_2O_3	0.16–2.44	1.17	0.54	0.78–1.69	1.06	0.32
FeO	0.05–0.18	0.11	0.04	0.03–0.11	0.06	0.03
MgO	0.05–0.10	0.07	0.01	0.05–0.07	0.06	0.01
Na_2O	0.02–0.14	0.08	0.03	0.04–0.10	0.06	0.02
Sc_2O_3	nd–0.08	0.05	0.02	nd–0.08	nd	nd
Cr_2O_3	nd–0.30	0.13	0.09	0.17–0.33	0.26	0.06
H_2O^b	0.85–0.96	0.91	0.02	0.87–0.92	0.89	0.02
Total	99.52–100.87	100.13	0.38	99.53–100.06	99.83	0.20

^a Total iron is shown as FeO . The detection limit for Sc_2O_3 is ~ 0.05 wt.%, and for Cr_2O_3 is ~ 0.06 wt.%. Abbreviations: Std. dev. = standard deviation, nd = not detected.

^b BeO and H_2O were calculated, not measured.

TABLE 2. Chemical composition of three Byrud emeralds, obtained by LA-ICP-MS.^a

Element (ppm)	Sample 203.18		Sample 195.174		Sample 106.718		DL (ppm)
	Range	Average	Range	Average	Range	Average	
Li	20–28	24	15–21	18	17–19	18	0.8
Mg	277–474	389	306–486	386	348–488	395	3.8
K	23–92	55	26–684	199	63–98	82	23
Sc	126–332	266	160–278	202	146–195	175	0.2
Ti	23–270	146	12–16	14	14–21	18	0.2
V	4965–10021	7356	4496–6895	5485	1745–4211	3098	1.1
Cr	293–1208	579	1006–1654	1324	162–932	585	1.8
Mn	5–25	5737	18–25	22	33–109	67	0.7
Fe	573–1024	802	467–698	576	570–881	719	5.8
Ni	nd	nd	nd	nd	nd–1	nd	0.5
Zn	9–15	5291	15–23	18	13–45	33	1.1
Ga	9–27	5841	19–26	23	nd	nd	0.3
Rb	29–61	41	21–54	32	26–33	30	0.4
Sr	nd	nd	nd–7	3	nd–8	4	1.9
Zr	nd–1.1	nd	nd–1	nd	nd–1	nd	0.4
Cs	50–127	85	35–44	38	69–99	85	0.4
Pb	1.8–2.8	2.2	3–5	4.25	5–14	8.67	0.01
V/Cr	6–24.3	16.2	3.68–4.47	4.18	4.52–10.8	6.79	
V/(V+Cr)	0.9–1	0.9	0.79–0.82	0.81	0.82–0.92	0.86	
Fe/(Fe+Cr)	0.4–0.8	0.6	0.24–0.41	0.31	0.49–0.78	0.60	

^a Co, Cu, La, Ce, Gd, Th, and U were analyzed for but not detected. Na, Cl, F, P, and Ca could not be analyzed correctly by this technique. Si is taken as the reference at 650,000 ppm. Abbreviations: DL = detection limit, nd = not detected.

DISCUSSION

Variations in Properties. The RI, SG, pleochroism, and fluorescence of our Byrud emeralds samples fall within the range of properties for emerald (Zylbermann, 1998). Higher values of RI were previously reported for Byrud emeralds ($n_o = 1.591$, $n_e = 1.584$; Webster, 1955).

Variations in color zonation, RI values, inclusion composition, and chemical composition may indicate that the mineralizing fluid was less homogeneous than is usual for emerald deposits. The relatively high concentration of chromophores (mostly V) may explain the high RI values sometimes observed, because—for example—V, which is heav-

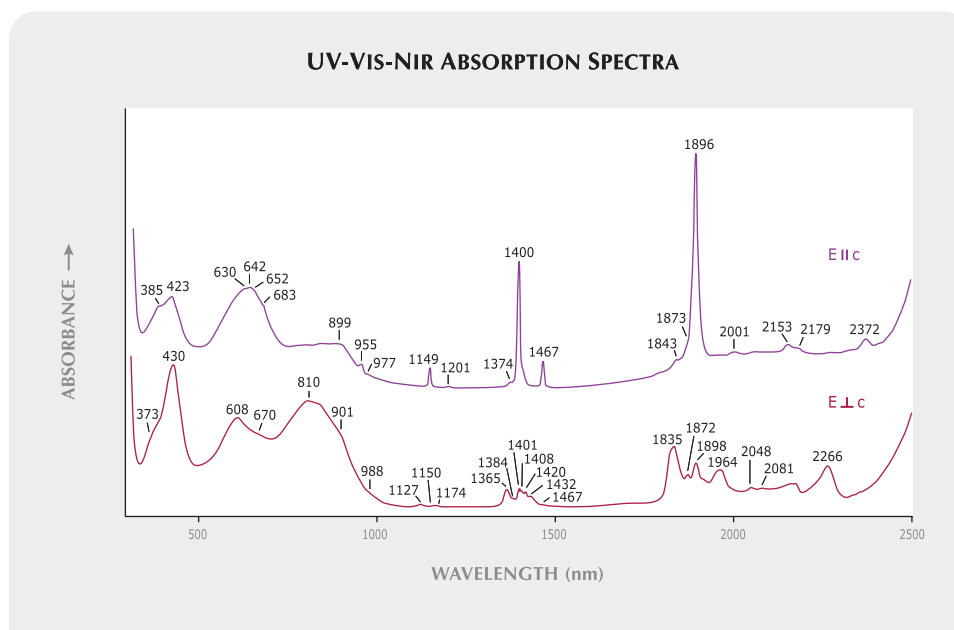


Figure 14. Polarized UV-Vis-NIR spectra of sample BVM2378-A show absorption bands at 430 and 608 nm (bottom) and 423 and 630–642 nm (top) that are due mostly to V^{3+} , and partly to Cr^{3+} . The weak shoulders at 385 (top) and 373 nm (bottom) are due to small amounts of Fe^{3+} . The sharp near-infrared peaks at approximately 1150, 1400, and 1896 nm are due to type II molecular water. Spectra have been shifted vertically for clarity. Sample thickness is 3 mm.

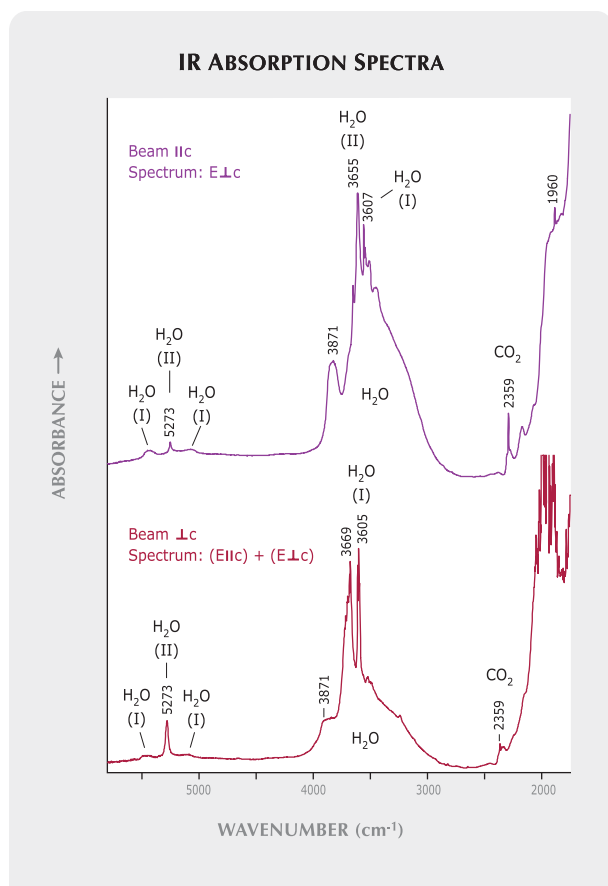


Figure 15. The IR spectra of Byrud emeralds clearly show absorptions due to H₂O and CO₂. Spectra have been shifted vertically for clarity.

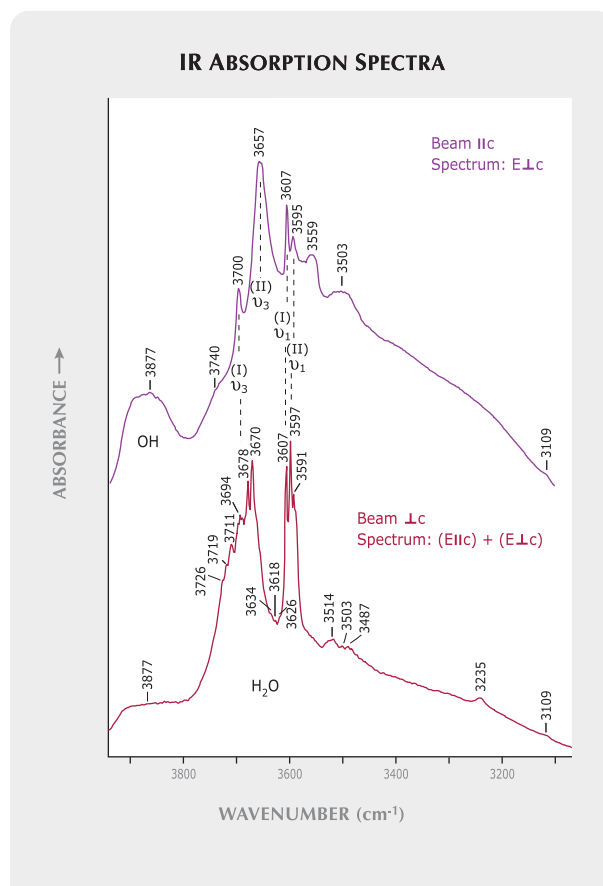


Figure 16. These IR spectra of emerald sample 195.174 in the 4000–3000 cm⁻¹ range show the details of water-related absorptions. Spectra have been shifted vertically for clarity.

ier than the Al it substitutes for, may contribute to slowing down light as it passes through the emerald. However, the RI values are sometimes very low, as seen in samples BVM2378–A to D, which were not chemically analyzed. Their low RI values may be related to the water and CO₂ content in the channels of these emeralds, which are very low compared to those of other natural emeralds (B. Sabot, pers. comm., 2006; a value of 1.1 wt.% H₂O is given by Alexandrov et al., 2001). As these samples were vivid green, the channel content apparently may be more important than the chromophores for controlling RI. Nevertheless, our limited data set does not allow us to demonstrate a clear correlation between RI and water, CO₂, and V contents.

Some solids in the multiphase inclusions were identified only with Raman spectroscopy (calcite) and others only with EDS (sylvite and pretulite), simply because we did not analyze the same specimens with both methods. This illustrates the diversity of the solid phases in the multiphase inclusions. However, opaque, metallic-appearing sulfides

were observed in the fluid inclusions of all seven samples studied.

Origin of Color. The main UV-Vis spectroscopic features are the absorption bands at 423 or 430 nm and at 608 or 642 nm. These positions prove that the color is due mainly to the presence of V. However, the weak peak at 683 nm indicates that Cr also contributes to the coloration. This was confirmed by chemical analyses: V was much more abundant than Cr.

Source of Vanadium and Chromium. Chromium in emerald typically originates from mafic and ultramafic rocks (e.g., Morteani and Grundmann, 1977; Laurs et al., 1996; Marshall et al., 2003), with the exception of Colombian-type deposits, where chromium is leached from sedimentary rocks (Giuliani, 1997). However, the geologic source of vanadium in emerald is not well documented. This element is usually concentrated in rocks that contain iron-rich

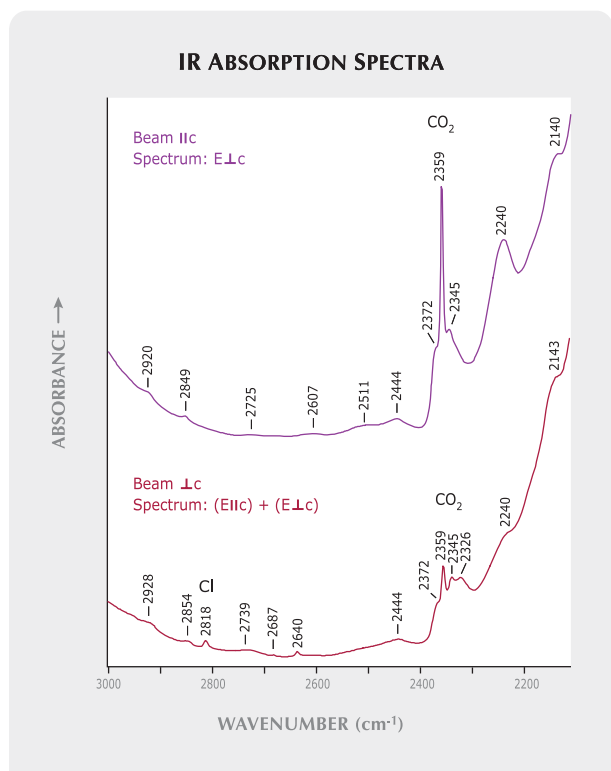
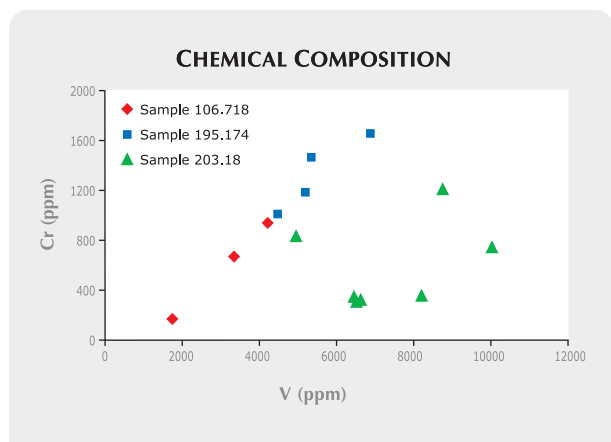


Figure 17. These IR spectra of emerald sample 195.174 in the 3000–2100 cm^{-1} range show the details of CO_2 -related absorptions. Spectra have been shifted vertically for clarity.

minerals or organic compounds (e.g., Moskalyk and Alfantazi, 2003). Byrud’s alum shales, rich in organic matter, are the most likely source of vanadium for these emeralds. By comparison, the source of

Figure 18. The contents of Cr and V in emeralds from Norway do not show a consistent correlation in the three Byrud emeralds tested.

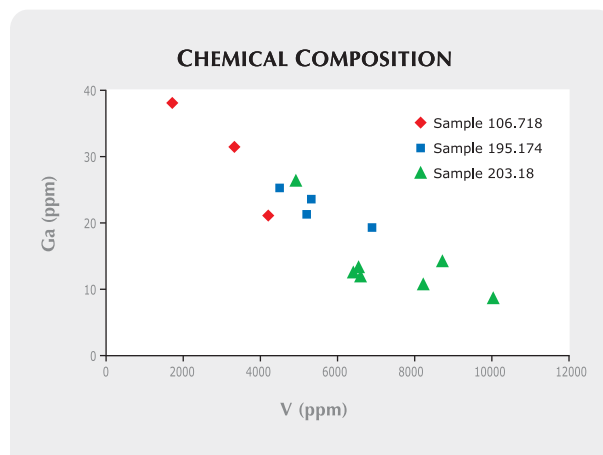


vanadium in Colombian deposits is also related to organic matter in black shales (Campos Alvarez and Roser, 2007).

Trace-Element Geochemistry. Trace-element incorporation into beryl varies with geologic environment (Staatz et al., 1965; Calligaro et al., 2000). We plotted some trace-element pairs to detect possible correlations in their relative abundances within the three samples analyzed. Chromium and V showed a positive correlation (figure 18) in two samples but not in sample 203.18. Gallium and V showed a clear negative correlation in all three samples (figure 19). A less pronounced negative correlation was found for Zn, Pb, and Mn relative to V (figure 20). From these data (based on the analysis of only three samples, as mentioned above), the group of divalent ions Zn, Mn, Pb, and Ga seems to correlate negatively with V, but we did not observe any correlation with Cr. All this confirms that Cr and V do not have similar geochemical distribution properties. Also, this could indicate that Ga and V integrate into the beryl structure via the same crystallographic site.

We calculated a very low water content in our samples (0.85–0.96 wt.%). This is not inconsistent with the value of 1.1 wt.% reported by Alexandrov et al. (2001). It approaches the lowest water content recorded for emerald from any source (Schwarz, 1987, p. 43). The low water content in such emeralds is related to the very low amount of Na, as type II water incorporation directly correlates to Na concentration (Wood and Nassau, 1968; Charoy, 1998).

Figure 19. The concentrations of Ga and V clearly show a negative correlation in all three Byrud samples.



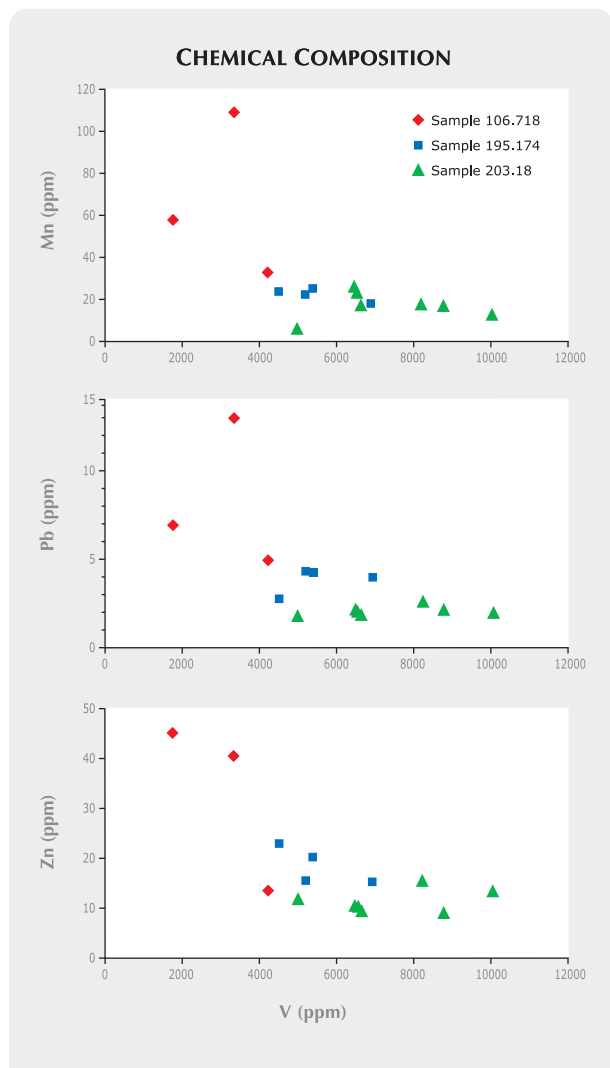


Figure 20. Concentrations of Mn, Pb, and Zn show a poorly pronounced negative correlation with V in the three Byrud emeralds.

IDENTIFICATION

We found several distinguishing criteria for Byrud emeralds. Most importantly, the presence of sulfides in the multiphase fluid inclusions is unique to emeralds from this locality and makes them straightforward to identify. With the optical microscope, we consistently observed a small (sometimes very small) black, opaque point somewhere in each multiphase inclusion. Three-phase and multiphase inclusions are known in emeralds from only a few other deposits: Colombia, Kaduna in Nigeria (Schwarz, 1998; Vapnik and Moroz, 2000; Sabot et al., 2000), Panjshir in Afghanistan (Seal, 1989; Bowersox et al., 1991), Kafubu in Zambia (Zwaan et al., 2005), and Xinjiang in China (Blauwet et al.,

2005). Multiphase inclusions in these emeralds commonly contain halite cubes and sometimes carbonate crystals, but none of them systematically show the black, opaque phases seen in emeralds from Byrud. Sulfides have been described as solid inclusions in emeralds from several deposits (Giuliani et al., 1997; Rondeau et al., 2003), but never as part of a multiphase inclusion. Also, we observed that fluid inclusions in Norwegian emeralds are generally more regular in shape than those in Colombian emeralds, and the halite cube they contain is smaller. Hence, the careful use of a binocular microscope can be sufficient to ascribe Norwegian provenance to an emerald.

Among chemical criteria, the very low Na concentration (about 0.1 wt.% or less) is most significant. This is comparable to emeralds from Emmaville, Australia (Schwarz, 1998), and Delbetey, Kazakhstan (Gravilenko et al., 2006), and is therefore not distinctive but certainly indicative. The appropriate data can be obtained by using either an electron microprobe or LA-ICP-MS.

In addition, the V content of the Byrud emeralds we tested was commonly high (a mean of more than 1 wt.% V_2O_3 , with values ranging up to 2.4 wt.%), which is consistent with earlier data (Schwarz, 1991; Calligaro et al., 2000). This is among the highest of all emeralds, along with those from Malipo, China (Zhang and Lan, 1999). However, the V content is sometimes lower (down to 0.16 wt.% V_2O_3), particularly in light green stones, so this criterion cannot be considered a definitive identification tool. Moreover, a high V/Cr ratio (3 to 24 in our measurements) is not distinctive: Emeralds from other deposits (Salininha, Brazil, and Lened, Canada) also can show high V/Cr ratios, sometimes exceeding 100 (Marshall et al., 2004). However, the relative contents of Fe+Mg (low), Cr (low), and Cs or Rb (high) appear specific to the emeralds from Byrud, as shown in a ternary diagram that plots Fe+Mg, Cr, and Cs (figure 21). The trace-element composition of emeralds from Lened (Canada) has not yet been determined, but it may be useful to compare it to Byrud in this ternary diagram.

The oxygen isotopic composition of an emerald from Byrud has been reported in the literature (Giuliani et al., 1998; Groat et al., 2002). The $\delta^{18}O$ value of 9.4‰ is rather low, but overlaps that of many other deposits (Giuliani et al., 1998; Sabot, 2002), so this criterion alone is not distinctive.

According to the published literature, the emeralds from Emmaville and Torrington, Australia, share

many characteristics with emeralds from Byrud (Schwarz, 1991). They formed in pegmatite sills that intruded alum schist (Schwarz, 1991, and references therein; Grundmann and Giuliani, 2002), and their associated minerals include quartz, feldspars, micas, fluorite, topaz, cassiterite, wolframite, and arsenopyrite. These Australian emeralds contain very low concentrations of Na₂O and MgO (<0.1 wt.%; Schwarz and Henn, 1992; Brown, 1998). Such low concentrations are otherwise encountered only in emeralds from Byrud and in synthetic emeralds. Emerald crystals from Emmaville and Torrington typically show strong color zonation parallel to the basal face, which is rare in emeralds from Byrud. Also, emeralds from Emmaville contain more chromium and less vanadium (0.1 wt.% V₂O₃) than those from Byrud (Schwarz, 1991).

CONCLUSION

The gemological and spectroscopic properties of our Byrud samples did not differ on average from those of emeralds in general, either chromium- or vanadium-bearing. However, our study has shown that

Figure 21. The chemical composition field of the three analyzed emeralds from Norway is clearly distinct from that of V-rich emeralds from other deposits. The elements used in this diagram (Cr, Fe + Mg, and Cs) are the most useful for distinguishing their geographic origins (data from Peucat et al., in preparation).

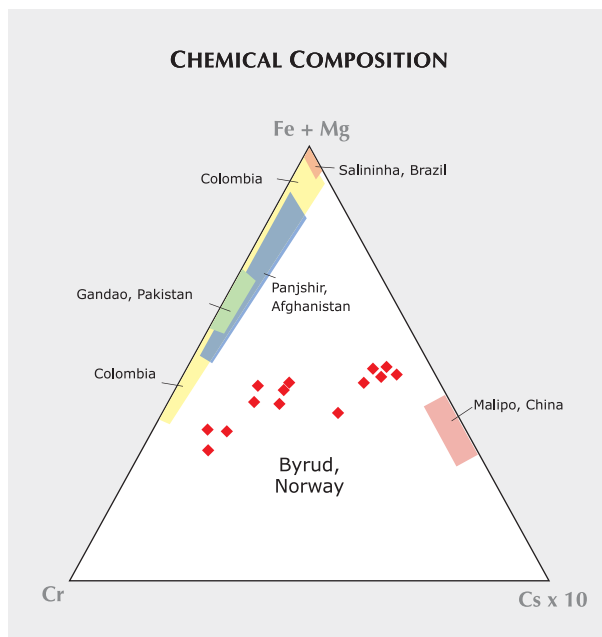


Figure 22. Significant quantities of emerald were mined from Byrud, Norway, in the late 19th and early 20th centuries. As these two crystals (9.6 and 5.5 mm long) illustrate, some of the material was transparent enough for faceting. Courtesy of the Royal Ontario Museum, Toronto; photo by Robert Weldon.

Byrud emeralds (e.g., figure 22) are colored mostly by vanadium. We also found a number of criteria that are diagnostic of these emeralds. Most importantly, we noted the presence of sulfide phases in multiphase fluid inclusions, together with halite, sylvite, calcite, liquid water, and gaseous CH₄. This is the first time that sulfide phases have been reported in multiphase inclusions in emeralds. They are seen with the optical microscope as minute black, opaque points. The chemical composition is also distinctive: The emeralds analyzed from Byrud had relative contents of Fe, Mg, Cr, Cs, and Rb that are specific to this locality and easily identified through LA-ICP-MS analysis. They also contained low Na and Mg and often high V.

These criteria make emeralds from Byrud unique and quite easy to distinguish using a microscope and/or chemical analysis. An unverified legend says that one of the emeralds in the jewels belonging to the British royal family comes from the Byrud deposit. Using the identification criteria provided in this article, it would now be quite easy to investigate this story.

When we compare our results with those reported in the literature for emeralds from other localities, it appears that those emeralds from Byrud that show a strong color zonation closely resemble emeralds from

Emmaville and Torrington, Australia: similar color zonation, very low Na and Mg contents, similar geologic setting, and similar associated minerals. Hence, a detailed gemological study of emeralds from Australia would be very helpful in testing the identi-

fication criteria proposed here for the emeralds from Byrud. In general, much remains to be done on vanadium-bearing emeralds (except perhaps for some Colombian deposits), which are much less studied than their chromium-bearing counterparts.

ABOUT THE AUTHORS

Dr. Rondeau (benjamin.rondeau@univ-nantes.fr) is assistant professor at the Laboratoire de Planétologie et Géodynamique, University of Nantes, France, and belongs to the Centre National de la Recherche Scientifique (CNRS), Team 6112. Dr. Fritsch is professor of physics at the University of Nantes, Institut des Matériaux Jean Rouxel (IMN)-CNRS. Dr. Peucat is a researcher in geochemistry at Géosciences Rennes, University of Rennes, France. Mr. Nordrum is curator at the Norwegian Mining Museum in Kongsberg, Norway. Dr. Groat is professor of mineralogy in the Department of Earth and Ocean Sciences, University of British Columbia, Vancouver, B.C., Canada.

ACKNOWLEDGMENTS

The authors are grateful to Mrs. M. Bouhnik-Le Coz (Géosciences Rennes) for performing LA-ICP-MS analyses. Special thanks to Dr. Bruno Sabot (Brioude, France) and Dr. Gaston Giuliani (INPG, Nancy, France) for their constructive comments on an early version of this article. Gunnar Raade (Oslo, Norway) kindly provided geological and mineralogical information, and Burny Iversen (Elverum, Norway), Atle Bergset (Langevåg, Norway), Knut Arne Eikrem (Grimstad, Norway), and Anne Grete Røise (Byrud farm, Eidsvoll, Norway) generously supplied historical background. Dr. Hanco Zwaan (National Museum of Natural History, Leiden, The Netherlands) is thanked for reviewing the original manuscript.

REFERENCES

- Alexandrov P., Giuliani G., Zimmermann J.-L. (2001) Mineralogy, age and fluid geochemistry of the Rila emerald deposit, Bulgaria. *Economic Geology*, Vol. 96, pp. 1469–1476.
- Blauwet D., Quinn E.P., Muhlmeister S. (2005) Gem News International: New emerald deposit in Xinjiang, China. *Gems & Gemology*, Vol. 41, No. 1, pp. 56–57.
- Bosshart G. (1991) Emeralds from Colombia (Part 2). *Journal of Gemmology*, Vol. 22, No. 7, pp. 409–425.
- Bowersox G., Snee L.W., Foord E.E., Seal II R.R. (1991) Emeralds of the Panjshir Valley, Afghanistan. *Gems & Gemology*, Vol. 27, No. 1, pp. 26–39.
- Brown G. (1998) Les gisements d'émeraude en Australie [Emerald deposits in Australia]. In D. Giard, G. Giuliani, A. Cheillett, E. Fritsch, and E. Gonthier, Eds., *L'émeraude*, Association Française de Gemmologie, Paris, pp. 201–204 [in French].
- Bull E. (1952) Bygdehistorien 1800–1914. *Eidsvoll bygds historie* [History of the Eidsvoll Parish]. Vol. 1, Part 2, p. 537 [in Norwegian].
- Burns R.G. (1993) *Mineralogical Applications of Crystal Field Theory*, 2nd ed. Cambridge Topics in Mineral Physics and Chemistry, Vol. 5. Cambridge University Press, Cambridge, UK.
- Calligaro T., Dran J.-C., Poirot J.-P., Quéré G., Salomon J., Zwaan J.C. (2000) PIXE/PIGE characterization of emeralds using an external micro-beam. *Nuclear Instruments and Methods in Physics Research B*, Vol. 161–163, pp. 769–774.
- Cameron E.A. (1963) Skattejaktminner fra Minnesund [Memories of a treasure hunt at Minnesund]. *Kvinner og Klær*, Vol. 40, pp. 33–54 [in Norwegian].
- Campos Alvarez N.O., Roser B.P. (2007) Geochemistry of black shales from the Lower Cretaceous Paja Formation, Eastern Cordillera, Colombia: Source weathering, provenance, and tectonic setting. *Journal of South American Earth Sciences*, Vol. 23, No. 4, pp. 271–289.
- Charoy B. (1998) Cristallochimie du béryl: L'état des connaissances [Beryl crystallochemistry: State of the art]. In D. Giard, G. Giuliani, A. Cheillett, E. Fritsch, and E. Gonthier, Eds., *L'émeraude*, Association Française de Gemmologie, Paris, France, pp. 33–39 [in French].
- CIBJO (1988) *Gemstone Book*. CIBJO Coloured Stones Commission, International Confederation of Jewellery, Silverware, Diamonds, Pearls and Gemstones, The Hague, Netherlands.
- Fritsch E., Moon M., Wu T.S.-T., Liu Y., Park J.S. (1998) Les nouvelles émeraudes synthétiques d'Asie: Émeraude synthétique hydrothermale chinoise, émeraudes synthétiques par dissolution anhydre coréenne et taïwanaise [New Asian synthetic emeralds: Hydrothermal synthetic emeralds from China, anhydrous dissolution synthetic emeralds from Korea and Taiwan]. In D. Giard, G. Giuliani, A. Cheillett, E. Fritsch, and E. Gonthier, Eds., *L'émeraude*, Association Française de Gemmologie, Paris, France, pp. 131–138 [in French].
- Fritsch E., Rondeau B., Notari F., Michelou J.-C., Devouard B., Peucat J.-J., Chalain J.-P., Lulzac Y., De Narvaez D., Arboleda C. (2002) Les nouvelles mines d'émeraude de La Pita (Colombie), 2de partie [The new emerald mines at La Pita, Colombia]. *Revue de Gemmologie a.f.g.*, No. 144, pp. 13–19 [in French].
- Giuliani G. (1997) Genèse des gisements d'émeraude du Brésil et de Colombie [Origin of emerald deposits in Brazil and Colombia]. Thèse d'Habilitation, Institut National Polytechnique de Lorraine, Nancy, France, 147 pp. [in French].
- Giuliani G., Cheillett A., Zimmermann J.-L., Ribeiro-Althoff A.-M., France-Lanord C., Feraud G. (1997) Les gisements d'émeraude du Brésil: genèse et typologie [Emerald deposits in Brazil: genesis and typology]. *Chronique Recherche Minière*, Vol. 526, pp. 17–61 [in French].
- Giuliani G., France-Lanord C., Coget P., Schwarz D., Cheillett A., Branquet Y., Giard D., Martin-Izard A., Alexandrov P., Piat D.H. (1998) Oxygen isotope systematics of emerald: Relevance for its origin and geological significance. *Mineralium Deposita*, Vol. 33, pp. 513–519.
- Goldschmidt V.M. (1911) Die Kontaktmetamorphose im Kristianiagebiet [Contact metamorphism in the Oslo region]. *Videnskapselskapets Skrifter, I. Matematisk-naturvitenskapelig klasse*, Vol. 1, pp. 56, 357–358 [in German].

- Gravilenko E.V., Calvo Pérez B., Castroviejo Bolibar R., Garcia del Amo D. (2006) Emeralds from the Delbegetey deposit (Kazakhstan): Mineralogical characteristics and fluid-inclusion study. *Mineralogical Magazine*, Vol. 70, No. 2, pp. 159–173.
- Groat L.A., Marshall D.D., Giuliani G., Murphy D.C., Piercey S.J., Jambor L., Mortensen J.K., Ercit T.S., Gault R.A., Matthey D.P., Schwarz D., Maluski H., Wise M.A., Wengzynowski W., Eaton D.W. (2002) Mineralogical and geochemical study of the Regal Ridge emerald showing, southeastern Yukon. *Canadian Mineralogist*, Vol. 40, pp. 1313–1338.
- Grundmann G., Giuliani G. (2002) Emeralds of the world. In G. Giuliani et al., Eds., *Emeralds of the World*, extraLapis English No. 2, pp. 24–35.
- Ihlen P.M. (1978) Ore deposits in the north-eastern part of the Oslo region and in the adjacent Precambrian areas. In E.-R. R. Neumann and I. B. Ramberg, Eds., *Petrology and Geochemistry of Continental Rifts*, Proceedings of the NATO Advanced Study Institute, Oslo, July 27–August 5, 1977, D. Reidel Pub. Co., Dordrecht, Netherlands, pp. 277–286.
- Kunz G.F. (1902) Precious stones. *Mineral Resources of the U.S. 1901*, U.S. Geological Survey, Bureau of Mines, Washington DC, pp. 729–771.
- Kvamsdal L., Eldjarn K. (2007) Mineralene i smaragdgruvene ved Byrud gård, Minnesund, Norge [The minerals in the emerald mines at Byrud farm, Minnesund, Norway]. *Stein*, Vol. 33, No. 4, pp. 4–20 [in Norwegian].
- Laurs B.M., Dilles J.H., Snee L.W. (1996) Emerald mineralization and metasomatism of amphibolite, Khaltaro granitic pegmatite-hydrothermal vein system, Haramosh Mountains, northern Pakistan. *Canadian Mineralogist*, Vol. 34, pp. 1253–1286.
- Lindaas K.D. (1982) Gruvedrift etter smaragd på Byrud Minnesund [Mining for emerald at Byrud Minnesund]. *Romerikstun*, Romerike historielag Årbok 1982, pp. 90–93 [in Norwegian].
- Marshall D., Groat L.A., Giuliani G., Murphy D., Matthey D., Ercit T.S., Wise M.A., Wengzynowski W., Eaton W.D. (2003) Pressure, temperature and fluid conditions during emerald precipitation, southeastern Yukon, Canada: Fluid inclusion and stable isotope evidence. *Chemical Geology*, Vol. 194, pp. 187–199.
- Marshall D., Groat L.A., Falck H., Giuliani G., Neufeld H. (2004) The Lened emerald prospect, Northwest Territories, Canada: Insights from fluid inclusions and stable isotopes, with implications for Northern Cordilleran emerald. *Canadian Mineralogist*, Vol. 42, pp. 1523–1539.
- Morteani G., Grundmann G. (1977) The emerald porphyroblasts in the penninic rocks of the central Tauern Window. *Neues Jahrbuch für Mineralogie Monatshefte*, Vol. 11, pp. 509–516.
- Moskalyk R.R., Alfantazi A.M. (2003) Processing of vanadium: A review. *Minerals Engineering*, Vol. 16, pp. 793–805.
- Nordrum F.S., Raade G. (2006) Das Smaragd-Vorkommen von Byrud (Eidsvoll) in Süd-Norwegen [The emerald deposit at Byrud (Eidsvoll) in South Norway]. *Mineralien-Welt*, Vol. 17, No. 4, pp. 52–64 [in German].
- Pouchou J.-L., Pichoir F. (1991) Quantitative analysis of homogeneous or stratified microvolumes applying the model “PAP.” In K.F.J. Heinrich and D.E. Newbury, Eds., *Electron Probe Quantitation*, Plenum Press, New York, pp. 31–75.
- Rondeau B., Notari F., Giuliani G., Michelou J.-C., Martins S., Fritsch E., Respingier A. (2003) La mine de Piteiras, Minas Gerais, nouvelle source d'émeraude de belle qualité au Brésil [The Piteiras mine, Minas Gerais, a new source of gem-quality emerald in Brazil]. *Revue de Gemmologie a.f.g.*, No. 148, pp. 9–25 [in French].
- Sabot B., Cheillettz A., de Donato P., Banks D., Levresse G., Barres O. (2000) Afghan emeralds face Colombian cousins. *Chroniques de la Recherche Minière*, Vol. 541, pp. 111–114.
- Sabot B. (2002) Classification des gisements d'émeraude: Apports des études pétrographiques, minéralogiques et géochimiques [Classification of Emerald Deposits: Highlights of Petrographical, Mineralogical and Geochemical Studies]. PhD thesis, Institut National Polytechnique de Lorraine, Nancy, France, 172 pp. [in French].
- Schmetzer K., Kiefert L., Bernhardt H.-J., Beili Z. (1997) Characterization of Chinese hydrothermal synthetic emerald. *Gems & Gemology*, Vol. 33, No. 4, pp. 276–291.
- Schwarz D. (1987) *Esmeraldas: Inclusões em Gemas [Emeralds: Inclusions in Gems]*. Imprensa Universitaria Universidad Federal de Ouro Preto, Ouro Preto, Brazil, 439 pp.
- Schwarz D. (1991) Die chemischen Eigenschaften der Smaragde, II. Australien und Norwegen [Chemical properties of emerald, II. Australia and Norway]. *Zeitung der Deutschen Gemmologischen Gesellschaft*, Vol. 40, No. 1, pp. 39–66. [in German].
- Schwarz D. (1998) De l'importance des inclusions solides et fluides dans la caractérisation des émeraude naturelles et synthétiques [The importance of solid and fluid inclusions in the characterization of natural and synthetic emeralds]. In D. Giard, G. Giuliani, A. Cheillettz, E. Fritsch, and E. Gonthier, Eds., *L'émeraude*, Association Française de Gemmologie, Paris, France, pp. 71–80 [in French].
- Schwarz D., Henn U. (1992) Emeralds from Madagascar. *Journal of Gemmology*, Vol. 23, No. 3, pp. 140–149.
- Schwarz D., Schmetzer K. (2002) The definition of emerald: The green variety of beryl colored by chromium and/or vanadium. In G. Giuliani et al., Eds., *Emeralds of the World*, extraLapis English No. 2, pp. 74–78.
- Seal R.R. II (1989) A reconnaissance study of the fluid inclusion geochemistry of the emerald deposits of Pakistan and Afghanistan. In A. H. Kazmi and L. W. Snee, Eds., *Emeralds of Pakistan: Geology, Gemology and Genesis*, Van Nostrand Reinhold, New York, pp. 151–164.
- Selset R. (1963) Emerald locality on Mjøsa Lake, Norway. *Rocks & Minerals*, Vol. 38, pp. 608–609.
- Sinkankas J. (1981) *Emerald and Other Beryls*. Chilton Book Co., Radnor, PA, 665 pp.
- Staatz M.H., Griffiths W.R., Barnett P.R. (1965) Differences in the minor element composition of beryl in various environments. *American Mineralogist*, Vol. 50, pp. 1783–1795.
- Vapnik Y., Moroz I. (2000) Fluid inclusions in emerald from the Jos complex (central Nigeria). *Schweizerische Mineralogische und Petrographische Mitteilungen*, Vol. 80, No. 2, pp. 117–129.
- Vogt J.H.L. (1884) Undersøgelser ved den sydlige del af Mjøsen i 81 og 82 [Investigations at the southern part of Lake Mjøsen in 1881 and 1882]. *Nyt Magazin for Naturvidenskaberne*, Vol. 28, pp. 215–248 [in Norwegian].
- Websky M. (1876) Über Beryll von Eidsvoll in Norwegen [On beryl from Eidsvoll in Norway]. *Tschermak's Mineralogischen und Petrologischen Abteilungen*, Vol. 6, No. 2, pp. 117–118 [in German].
- Webster (1955) The emerald. *Journal of Gemmology*, Vol. 5, p. 303.
- Wood D.L., Nassau K. (1968) The characterization of beryl and emerald by visible and infrared absorption spectroscopy. *American Mineralogist*, Vol. 53, pp. 777–800.
- Zhang L., Lan Y. (1999) Gemological characteristics and deposit geology of Yunnan emerald. *Acta Mineralogica Sinica*, Vol. 19, No. 2 [in Chinese; no pagination].
- Zwaan J.C., Seifert A.V., Vrāna S., Laurs B.M., Anckar B., Simmons W.B., Falster A.U., Lustenhouwer W.J., Muhlmeister S., Koivula J.I., Garcia-Guillermine H. (2005) Emeralds from the Kafubu area, Zambia. *Gems & Gemology*, Vol. 41, No. 2, pp. 116–148.
- Zylbermann N. (1998) Tableau synoptique comparatif des propriétés gemmologiques des gisements majeurs et des principales synthèses [A comprehensive comparison of the gemological properties of major deposits and principal synthetics]. In D. Giard, G. Giuliani, A. Cheillettz, E. Fritsch, and E. Gonthier, Eds., *L'émeraude*, Association Française de Gemmologie, Paris, France, pp. 227–233 [in French].